

## Numerical Analysis of Severe Plastic Deformation by High Pressure Torsion

Mohammadreza kaji<sup>1</sup>, Ghader Faraji<sup>2\*</sup>

<sup>1</sup> Master Student, Department of Mechanical Engineering, College of Engineering, University of Tehran, Tehran, Iran.

<sup>2</sup> School of Mechanical Engineering, College of Engineering, University of Tehran, Tehran, 11155-4563, Iran.

---

### ARTICLE INFO

#### Article history:

Received 6 April 2016

Accepted 1 July 2016

Available online 15 July 2016

#### Keywords:

Finite element modeling

High pressure torsion (HPT)

Stress and strain distribution

---

### ABSTRACT

High-pressure torsion (HPT) is a metal processing method in which the sample is subjected to a very high plastic shear deformation. This process can produce exceptional levels of grain refinement, and provides a corresponding improvement in mechanical properties. To investigate the stress and strain distribution due to HPT process finite element simulation were conducted to investigate effective parameters. The simulation results demonstrate that the lowest effective strain obtained in the centers of the disk and the highest at the edges. Also, the mean stress varies linearly from the center of the disk to the edge region. The compressive stresses are higher in the disk centers and lower at the edges. By increasing the friction coefficient and the die angle, mean stress decrease and stress variation along the disc diameters become more homogeneous. Increasing of the pressure load leads to increase the mean stress and its heterogeneity along the disc radius.

---

### 1. Introduction

Metals with nano and submicron grain size have received much attention during the last decades because of their unique physical and mechanical properties [1]. Severe plastic deformation (SPD) methods have been extensively performed for producing ultrafine grained or nanostructured metals [2]. Recent studies have shown that high levels of plastic deformation have a significant influence on the microstructure and mechanical properties. Although severe plastic deformation processes lead to improving strength, it often reduces ductility [3]. Strengthening mechanism by severe plastic deformation is not still explain properly but it can be justified that severe plastic deformation processes reduce the grain size and according to Hall-Patch relation ( $\sigma = \sigma_0 + Kd^{-1/2}$ ), the strength increases [4]. Several SPD processes such as equal channel angular pressing (ECAP) [5], high-pressure torsion (HPT) [6], twist extrusion (TE) [7], accumulative roll-bonding (ARB) [8], tubular channel angular pressing [9], and repetitive forging [10] have received much interest as group of top-down techniques to produce bulk ultrafine grained and nanostructured metals. HPT was presented by Bridgman in 1935 [11], though the principles are now well established during the last two decades [6]. The sample in HPT is usually in the form of a small thin disk. During this process, the disk is subjected to a compressive load and concurrent torsional deformation. Because the friction in contact surfaces between the sample and the anvils, the sample is deformed by shear tension. The high

1/2), the strength increases [4]. Several SPD processes such as equal channel angular pressing (ECAP) [5], high-pressure torsion (HPT) [6], twist extrusion (TE) [7], accumulative roll-bonding (ARB) [8], tubular channel angular pressing [9], and repetitive forging [10] have received much interest as group of top-down techniques to produce bulk ultrafine grained and nanostructured metals. HPT was presented by Bridgman in 1935 [11], though the principles are now well established during the last two decades [6]. The sample in HPT is usually in the form of a small thin disk. During this process, the disk is subjected to a compressive load and concurrent torsional deformation. Because the friction in contact surfaces between the sample and the anvils, the sample is deformed by shear tension. The high

---

\* Corresponding author:

E-mail: ghfaraji@ut.ac.ir

imposed compressive hydrostatic pressure prevents any cracking of the sample and the low thickness to diameter ratio lead to the production of a high strain during anvil rotation [12].

The precise characteristics of HPT processing may be divided into three separate categories, depending upon the configuration of the anvil and consequent restrictions on the lateral flow of the material. These configurations are termed constrained, quasi-constrained and unconstrained [6]. In the unconstrained facility, lateral flow of the material is not eliminated. It is partially restricted in the quasi-constrained facility, and it is entirely restricted in the constrained facility. The grain refinement and the corresponding enhancement of mechanical properties obtained by an HPT process are to a largely dependent on the pressure and strain imposed on the material. In HPT process stress and strain distribution along the disc diameter are heterogeneous, so sample has non-uniform structure. Because of heterogeneity structure during HPT, mechanical property is similar to the evolution of effective strain during HPT. The distribution of the strain and the pressure in a sample are determined by the geometry and material of both the die and the sample, and the friction between die and sample [13].

The finite element method (FEM) is one of the most important numerical methods that can be used to explain the effect of the geometry and

material characteristics on the results of HPT process. Uniform strain distribution along the disc diameter could lead to homogeneous mechanical property. In the present study, the parameters that have an effect on the homogeneity of the structure were studied. The evolution of the sample shape, stress and strain during HPT and The effects of the friction coefficient, die angle, pressure load and the temperature evolution of the sample was investigated by FEM analysis.

## 2. Finite element simulation

Simulations were performed by using the FEM ABAQUS 6.13 software. Since there is axial symmetry around the central axis, the simulation was simplified by considering a two-dimensional axisymmetric model [14]. In practical work Semi constraint configuration due to impose hydrostatic pressure on a sample and need simple equipment are mostly used, so semi-constrained configuration have been considered for present simulation. The present simulations consider only the sample and bottom anvils. These components are present in all HPT facilities, although their shape and volume may vary. For the analyses, presented here, a disk-shaped specimen with diameter  $D = 10$  mm and thickness  $H = 1.0$  mm is selected. The die geometry is shown on Figure 1.

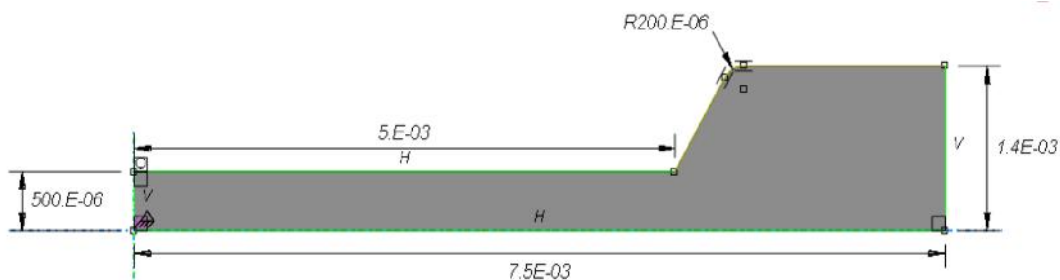


Fig 1. Geometry and dimensions of an axisymmetric section of the die.

The sample is modelled as soft iron. The mechanical and thermal characteristic that are used for sample listed in Table 1 [3]. The dies were modeled as bodies with extra high strength and module of elasticity. A coefficient of heat convection of  $50 \text{ Wm}^{-2}\text{K}^{-1}$  between the equipment and the environment and a coefficient of heat transfer of  $11 \text{ Wm}^{-1}\text{K}^{-1}$

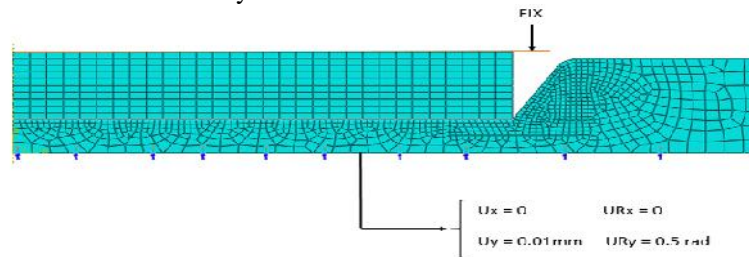
between the die and sample were used in the simulations to provide the best agreement with the real condition [12]. Coulomb frictional contact condition is applied at the interface between the steel sample and the dies. For the first simulation 1 GPa pressure load with 100 rad/s rotational rate during  $30^\circ$  rotation, considered for a bottom anvil.

**Table 1.** Mechanical and thermal properties had been used for present simulation [2].

Material	Young module (GPa)	Yield stress (MPa)	Density (Kgm <sup>-3</sup> )	Conductivity (Wm <sup>-1</sup> K <sup>-1</sup> )	Heat capacity (MJm <sup>-3</sup> K <sup>-1</sup> )
Iron	190	1000	7860	80	3.52

The suitable mass scale was used for the corner of the die to reduce the solving time and improve convergence. Due to high deformation, the sample cannot cope with the extreme plastic deformation. So Abaqus offers several tools to improve mesh quality in a simulation where severe mesh distortion are taken place. First: partitioning the outer edge of the die, to introduce more element in the vicinity of the

inclined line of die. A higher mesh density in this critical area improves the stability of the contact algorithm. Second: applying adaptive mesh to maintain reasonable element shapes and aspect ratios while the shape of the sample is evolving [15]. Both of techniques are used in the present work. In figure 2 the initial sample and die mesh condition is depicted.

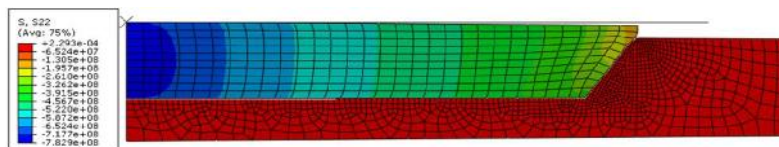
**Fig 2.** Boundary conditions used in finite element method.

### 3. Result and discussion

#### 3.1. Stress distribution

Figure 3 shows the distribution of stress along the cross section of the sample during HPT. Since the whole of the disc undergo pressure stress, the sign of the stress is negative. It is observed from the present simulations that there is notable variation in the mean stress distribution along the sample. It is demonstrated that the highest compressive stresses exist in the center of the disk, and there are less compressive stresses near the end of edges. Due to friction effects, the compressive stress is higher at the disk centers. The radial friction load may be estimated as a constant in contact areas between the sample and the die so that the edges of the samples experience only the back stress due to

the friction load. In the other hand, the inner regions of the sample experience the back stress due to the friction load of its area plus the back stress of the outer regions. This means that by increasing distance from the centers, the mean stresses decrease linearly. The simulation also demonstrates that if the rotation angle increase, the average compressive stress decreases. The reduction of the compressive stresses along the disc is attributed to the increase of the area of the extruded burr of metal between the dies. This significantly increases the area supporting the compressive load from the anvils. Figure 4 compares the distribution of the stress on the cross section for the present simulation with results of the reference [16] at the same condition to verify the results.

**Fig 3.** Stress distribution along the disc diameter after 1Gpa pressure and 30° turn.

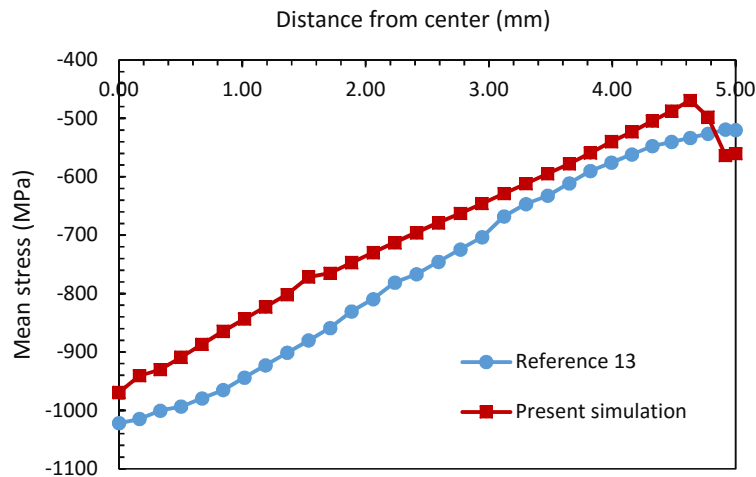


Fig. 4. Comparison of stress distribution along disc determined by present simulation and reference [13] to verify present simulation.

### 3.2. Strain distribution

The effective strain ( $\epsilon$ ) imposed on the disc is given by the relationship:

$$\epsilon = \frac{2\pi N}{h\sqrt{3}} = \frac{R\omega t}{h\sqrt{3}} \quad (2)$$

Where  $R$  is the distance to the center of the disc,  $N$  is the number of turns,  $h$  is the disk thickness,  $\omega$  is the rotation rate, and  $t$  is the time of processing [17]. The simulations demonstrate that the effective strains applied on the disc sample are highest at the edges and lowest in the centers of the disk. Figure 5 illustrates the distributions of the mean strains along the cross-sections for simulations with  $P=1.0$  GPa and rotation rate 100 rad/s. Also, strain distribution, depend on the thickness of sample and amount of rotation. It is observed that when the thickness increase, the mean strain decreases. Also, the effective strain increases with increasing the angle of rotation. The effective strain in the mid-plane is different from that in the top plane near

the edge. This strain heterogeneity in the top plane is because of the formation of a dead zone and the slope of the sidelong wall [18]. The effective strain at the midplane increases with  $r$ , while in the top plane the strain decreases with  $r$ . The reasons for this consist of strain gradient effect, geometric reasons, compressive deformation effect combined with the flash constraint, and also finite mesh size in FE modeling [19]. It should be noted that by increasing the effective strain, the dislocation density of the sample are increased. Also, the microstructure with smaller grain could be achieved. Dislocation density increases from a low value at the center to a maximum value at the edge. Because of heterogeneity structure during HPT, mechanical property such as hardness shows a similar trend with the change of effective strain. So, the hardness in the mid plane rises with the angle of rotation along the radial direction from the disk center [6].

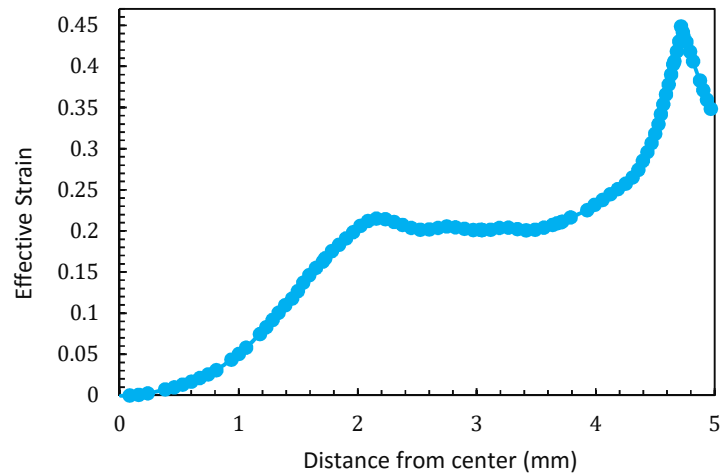


**Fig 5.** Effective (Von Mises) strain distribution along the disc diameters after 1GPa pressure and 30° turn.

### 3.3. Friction coefficient

The large normal compressive forces, due to high hydrostatic pressure, cause the large frictional force between the dies and the sample during HPT process. To investigate the effect of the friction coefficient on the HPT process, different friction coefficients (0.6, 0.5, 0.3 and 0.2) were considered. It was observed that the stress decrease continuously with increasing in the friction coefficients. The roughness of the die surface must be adequate to prevent slippage between the sample and dies. So, the friction between the die and the sample have to be

sufficient sticking condition. Therefore, the small friction coefficient is not desired. It should be noted that large friction coefficient could exacerbate the stress distribution and lead to strain heterogeneity. It could also be noted that the friction coefficient plays an important role to control the torque such that the frictional result may increase the torque required for HPT processing. Stress distribution along the disc diameter for different friction coefficients at 0.2 GPa pressure and 30° rotation are shown in figure 6.

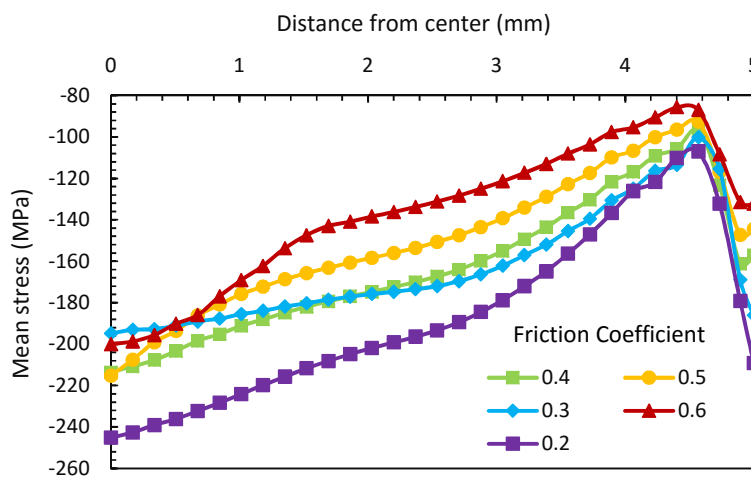


**Fig 6.** Stress distribution along disc with different friction coefficient.

### 3.4. Die angle

The shape of the die is a key factor to determine the homogeneity of the stresses and the distribution of the strains in the sample. The depth of the cavities in the symmetric dies in a semi-constrained configuration has to be large enough to guarantee radial containment of the sample, on the other hand, a too large depth can result in an undesirable contact of the dies at the end of the compression stage and/or during torsion. The depth of the sample cavity in the dies is chosen to be 0.9 mm. Next to the depth of

the die cavity, also the inclination angle of the lateral boundary is important since it affects both the level of hydrostatic pressure and strain distribution. For studying inclination angle influence on the stress distribution, two angles ( $120^\circ$ ,  $130^\circ$ ) were simulated. The distribution of stress along the disc diameters for two angles are shown in Figure 7. The results indicate that by an increase in the inclination angle, the mean stress decreases and stress variation along the disc diameters become more homogeneous.

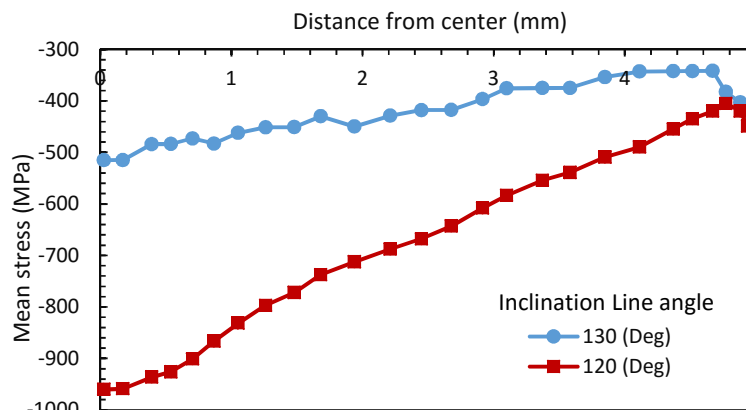


Fig. 7. Comparison of stress distribution along disc with different inclination line angle of  $120^\circ$  and  $130^\circ$ .

### 3.5. Pressure load

Pressure load in the present simulation was applied by vertical die displacement. Three displacement (0.01, 0.05 and 0.1mm) were considered. Stress distribution along the disc diameter are shown in figure 8 for three

displacements at the same rotation condition. It is clear from the simulation that increasing pressure load lead to increase mean stress and heterogeneity along the disc. Stress promotion in the central area of the disc are higher than in the corner area of the disc.

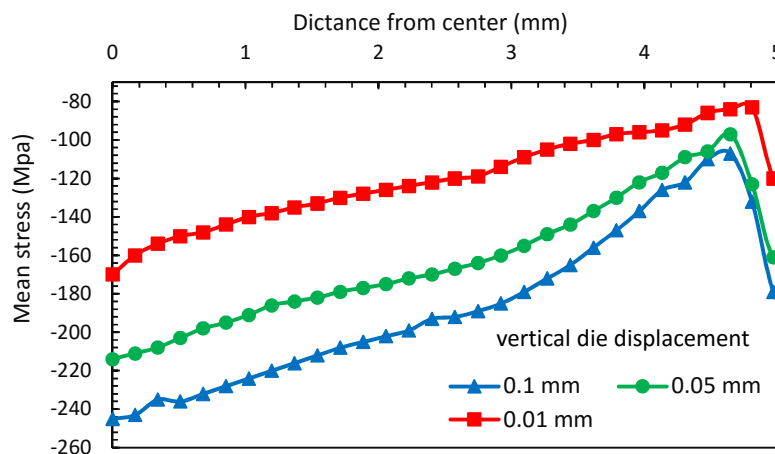


Fig. 8. Comparison of stress distribution along disc with different vertical die displacement.

### 3.6. Temperature distribution

The thermal characteristics of the disks especially the rise in the disk temperature is an important parameter in HPT processing. Because this will determine the potential for obtaining a high degree of grain refinement. The fundamental thermal characteristics of HPT processing can be simplified into three distinct parts: the heat source, the thermal conductivity resistance, and the heat sinks. The heat source is the plastic deformation of the sample. The thermal conductivity resistance derives from the conductivity of the material used for processing, the interface between the sample and the anvil, the conductivity of the anvil, the external conductivity to the HPT processing facility, the convection coefficients to the environment and the emissive coefficient. The heat sinks are the

heat capacities of the sample, the anvil, the HPT facility and the environment. The amount of heat generated by plastic deformation is usually considered to be a fraction of the plastic work imposed on the sample where the plastic work is the integral of the flow stress and the effective plastic strain.

Because the work of plastic deformation mainly converts to the heat, stress increasing in sample lead to increase temperature. Figure 10 show the evolution of the maximum temperature on the disk for the HPT processing of iron at different applied pressures of 1GPa and 2GPa. The simulations show that an increasing applied pressure leads to an increase in the temperature due to the increased volume of material outflow between the anvils.

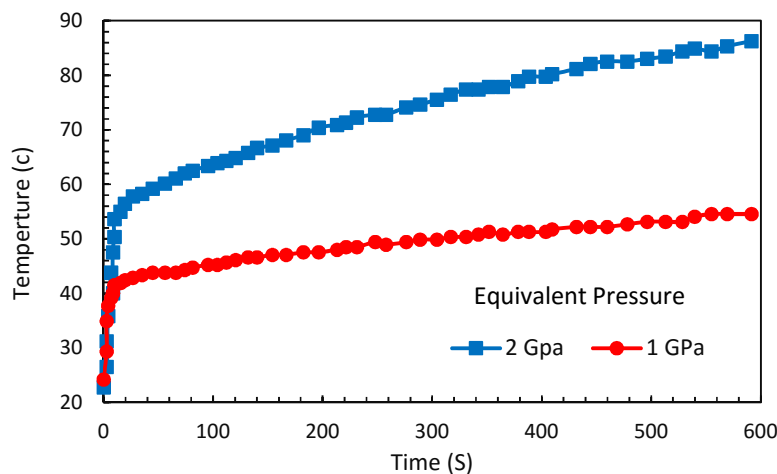


Fig. 9. Temperature evolution as a function of time at the different pressure.

### 4. Conclusion

In this study, simulations of the HPT process using the finite element code Abaqus are performed. The effects of various parameters were evaluated, including friction coefficient, die angle, pressure, and temperature rise. The mean stresses vary linearly from the center of the disk to the edge during HPT processing. Higher compressive stresses at the center and a lower one at the edge of the disk sample were observed. The different effective strains at the top plane and midplane were observed, and the strain decreases along the disc radius. By increasing friction coefficient, the amount of stress decreases consciously. If bigger angle

used for the die, stress heterogeneity increases. Increasing pressure load leads to increase in the mean stress and heterogeneity along the disc. Temperature rises more rapidly at the faster rotation rates and larger pressures.

### Acknowledgement

This work has been supported by the Center for International Scientific Studies & Collaboration (CISSC).

### References

- [1] G. Faraji, M. M. Mashhadi, S. H. Joo, H. S. Kim, "The role of friction in tubular channel

- angular pressing," *Rev. Adv. Mater. Sci.*, Vol. 31, 2012, pp. 12-18.
- [2] M. A. Meyers, A. Mishra, D.J. Benson, "Mechanical properties of nanocrystalline materials", *Prog. Mater. Sci.*, Vol. 51, 2006, pp. 427-556.
- [3] D. G. R. Willian D. Callister "Fundamental of materials science and engineering," 2010.
- [4] T.G.Langdon, "the processing of ultra fine-grained metal throught the application of several plastic deformation," *J. Mater. Sci.*, Vol. 47, 2007, pp. 211-216.
- [5] U. C. Patil Basavaraj V, T.S. Prasanna Kumarb, "Effect of geometric parameters on strain, strain inhomogeneity and peak pressure in equal channel angular pressing – A study based on 3D finite element analysis," *J. Manuf. Processes.*, Vol. 261, 2014, pp. 10-20.
- [6] T. G. L. Alexander P. Zhilyaev "Using high-pressure torsion for metal processing: Fundamentals and applications," *Prog. Mater. Sci.*, Vol. 53, 2008, pp. 893-979.
- [7] M. L. Jung, G. Kim, N. Pardis, Yan E. Beygelzimer, Hyoung Seop Kim, "Finite element analysis of the plastic deformation in tandem process of simple shear extrusion and twist extrusion," *Mater. Des.*, Vol. 83, 2015, pp. 858-865.
- [8] M. N. M. Reihanian, "An analytical approach for necking and fracture of hard layer during accumulative roll bonding (ARB) of metallic multilayer," *Mater. Des.*, Vol. 89, 2016, pp. 1213-1222.
- [9] G. Faraji, M. Ebrahimi, and A. R. Bushroa, "Ultrasonic assisted tubular channel angular pressing process," *Mater. Sci. Eng., A*, Vol. 599, 2014, pp. 10-15.
- [10] A. Babaei, G. Faraji, M. Mashhadi, and M. Hamdi, "Repetitive forging (RF) using inclined punches as a new bulk severe plastic deformation method," *Mater. Sci. Eng., A*, Vol. 558, 2012, pp. 150-157.
- [11] P. W. Bridgman, "Effects of High Shearing Stress Combined with High Hydrostatic Pressure," *Phys. Rev*, Vol. 48, 1935, pp. 825-850.
- [12] P. H. R. P. Roberto, B. Figueiredo, M. Teresa, P. Aguilar, "Using finite element modeling to examine the temperature distribution in quasi-constrained high-pressure torsion," *Acta Mater.*, Vol. 60, 2012, pp. 1390-3198.
- [13] C. G. John, J. Jonas, "The equivalent strain in high pressure torsion," *Mater. Sci. Eng., A*, Vol. 607, 2014, pp. 530-535.
- [14] G. Faraji, M. Mashhadi, A. Dizadji, and M. Hamdi, "A numerical and experimental study on tubular channel angular pressing (TCAP) process," *J. Mech. Sci. Technol.*, Vol. 26, 2012, pp. 3463-3468.
- [15] D. Systèmes, Abaqus Documentation, ed, 2009.
- [16] P. R. C. Roberto, B. Figueiredo, T. G. Langdon, "Using finite element modeling to examine the flow processes in quasi-constrained high-pressure torsion," *Mater. Sci. Eng., A*, Vol. 528, 2011, pp. 8198-8204.
- [17] H. S. L. Kim H.S , Lee.YS, "deformation behavior of copper during High Pressure Torsion Processing," *J. Mater. Process. Technol.*, Vol. 142, 2003, pp. 334-337.
- [18] E. Y. Y. Dong Jun Lee, S. H. Lee, S. Y. Kang , Hyoung Seop Kim, "FINITE ELEMENT ANALYSIS FOR COMPRESSION BEHAVIOR OF HIGH PRESSURE TORSION PROCESSING," *Rev. Adv. Mater*, Vol. 31, 2012, pp. 25-30.
- [19] E. Y. Y. Dong Jun Lee , D. H. Ahn , B. H. Park , H. W. Park , L. J. Park, "Dislocation density-based finite element analysis of large strain deformation behavior of copper under high-pressure torsion," *Acta Mater.*, Vol. 76, 2014, pp. 281-293.